Front. Chem. China 2009, 4(1): 93–103
DOI 10.1007/s11458-009-0018-7

RESEARCH ARTICLE

Xiangfeng LI, Chusheng LI, Jiang LU, Hui LIANG

Designed synthesis and chiroptical properties of regioregular poly(*p*-phenyleneethynylene-alter-m-phenyleneethynylene) bearing (-)-trans-myrtanoxyl side groups

Abstract Two regioregular poly(*p*-phenyleneethynylene-*alter*-*m*-phenyleneethynylene)s bearing (-)-*trans*-myrtanoxyl side groups with different substitution patterns were designed and synthesized, e.g. Myr-PMPE-1 and Myr-PMPE-2. In Myr-PMPE-1, the side chiral groups are distributed uniformly along the backbone. In Myr-PMPE-2, the distribution of the side chiral groups is alternatively crowded and loose. Both of these two polymers show no CD signal in solutions because of their good solubility. The investigations of chiroptical properties of these two polymers were carried out in the form of spin-coated films. The films were annealed above the glass temperature of the corresponding polymer, and the effects of annealing temperature and time on the properties of the films were investigated by UV-Vis absorption, fluorescence and circular dichroism spectra. The results show that annealing treatment had no significant effect on the properties of Myr-PMPE-1, including UV-Vis absorption, fluorescence and optical activity. The maximum absolute value of dissymmetry factor ($|g_{max}|$) was 1.62×10^{-4}. On the other hand, annealing treatment significantly affected the properties of Myr-PMPE-2. Without annealing or being annealed below 100°C, Myr-PMPE-2 films show almost no Cotton effect. In contrast, when annealed above 120°C, the absorption and emission of Myr-PMPE-2 films slightly red shifted with increasing annealing temperature and annealing time. Most importantly, the intensity of CD signals increased significantly and the optical activity of Myr-PMPE-2 films markedly increased. After annealing at 140°C for 4 h, the $|g_{max}|$ of Myr-PMPE-2 films was increased up to 3.07×10^{-3}, about one order of magnitude higher than that of Myr-PMPE-1 films.

Translated from *Acta Polymeric Sinica*, 2008, 3 (in Chinese)

Xiangfeng LI, Chusheng LI, Jiang LU, Hui LIANG (✉)
School of Chemistry and Chemical Engineering, Sun Yat-Sen University, Guangzhou 510275, China
E-mail: ceslhui@mail.sysu.edu.cn

Keywords chiral, conjugated polymer, optical activity, circular dichroism

Because of the combination of conjugated structure and optical activity, chiral conjugated polymers have potential applications in many fields such as chiral separations [1], enantioselective recognitions [2], surface-modification of electrodes [3], chemical and biological sensors [4], nonlinear optical materials [5] and circularly polarized luminescent (CPL) materials [6–8]. The reported chiral conjugated polymers can be divided into two groups: (1) Main chain chiral conjugated polymers, mainly conjugated polymers containing chiral binaphthylene moieties [9–14]; (2) Conjugated polymers with chiral side groups, including polythiophenes [6,15–18], poly(*p*-phenylenevinylene)s [7, 19,20], polyfluorenes [21–23], polyacetylenes [24,25], polysilylenes [26–28] and polycarbazoles [29] *etc*.

The optical activity of chiral conjugated polymers can be characterized with dissymmetry factor (g), which is defined as $g_{abs} = 2(\varepsilon_L - \varepsilon_R)/(\varepsilon_L + \varepsilon_R)$ .The optical activity of chiral conjugated polymers strongly depends on their molecular structure: (1) regioregularity is indispensable for the optical activity, more regular structure induces higher optical activity [6,20,30]; (2) the optical activity increases with increasing average enantiomerically pure pendant groups per monomeric unit [20]; (3) main chain liquid-crystallinity can significantly enhance optical activity [21]; (4) the introduction of intrinsically helical structure is more efficient to enhance the optical activity than the interchain helical organization [31,34]. Most of the chiral conjugated polymers show optical activity only under aggregation states, e.g. in poor solutions or in the solid state, but not in good solutions. The focus of this paper is to design and synthesize new chiral conjugated polymers and investigate the relationship between the optical activity and molecular structure of the obtained polymers.

In order to obtain polymers with regular molecular structure, it is essential to avoid isomerization reactions

during the polymerization. So, the Sonogashira reaction, which induces no isomer structure in the polymer, was selected to synthesize the polymers. The monomer structure was designed to ensure regioregular linking between monomeric units. Moreover, *m*-phenylene linkages were introduced to encourage intrinsically helical conformation [32]. Thus, two regioregular poly(*p*-phenyleneethynylene-*alter*-*m*-phenyleneethynylene)s bearing (-)-*trans*-myrtanoxyl side groups were designed and synthesized. These two polymers have the same chemical component and main chain structure, but the substitution pattern of the chiral groups is different from each other. The synthetic route is shown in Scheme 1.

1 Experiments

1.1 Materials and instruments

Iodic acid (HIO_3), ⩾99.5%, was from the Shanghai Xinliang Chemical Reagent Co Ltd; triphenylphosphine (PPh_3), CP was from the Sinopharm Chemical Reagent Co Ltd. CuI (98%), 2-methylbut-3-yn-2-ol (98%), 4-bromophenol (99%), aq. sodium hypochlorite (5% Cl) were all from Alfa Aesar Ltd. Sodium iodide (NaI), > 99.5% were from the Tianjin Damao Chemical Reagent Factory.

^{1}H-NMR spectra were recorded on a Mercury-Plus 300 NMR spectrometer (Varian) in $CDCl_3$ with tetramethylsilane as an internal standard. The molecular weights and molecular weight distributions (MWD) were determined by Waters-Breeze GPC in THF at room temperature on polystyrene gel columns (Waters styragel HR1, HR3, HR4) connected with a refractive index detector (RI-2417) using polystyrene standards for calibration. CD and UV-Vis spectra were recorded on a Jasco J-810 Circular Dichroism Spectrometer. Elemental analyses were carried out on a Vario EL Elemental Analyzer (Elementar). EI-mass measurements were carried out on a DSQ EI-mass spectrometer (Thermo). FAB-mass measurements were carried out on a VG ZAB-HS mass spectrometer. Differential scanning calorimetry (DSC) measurements

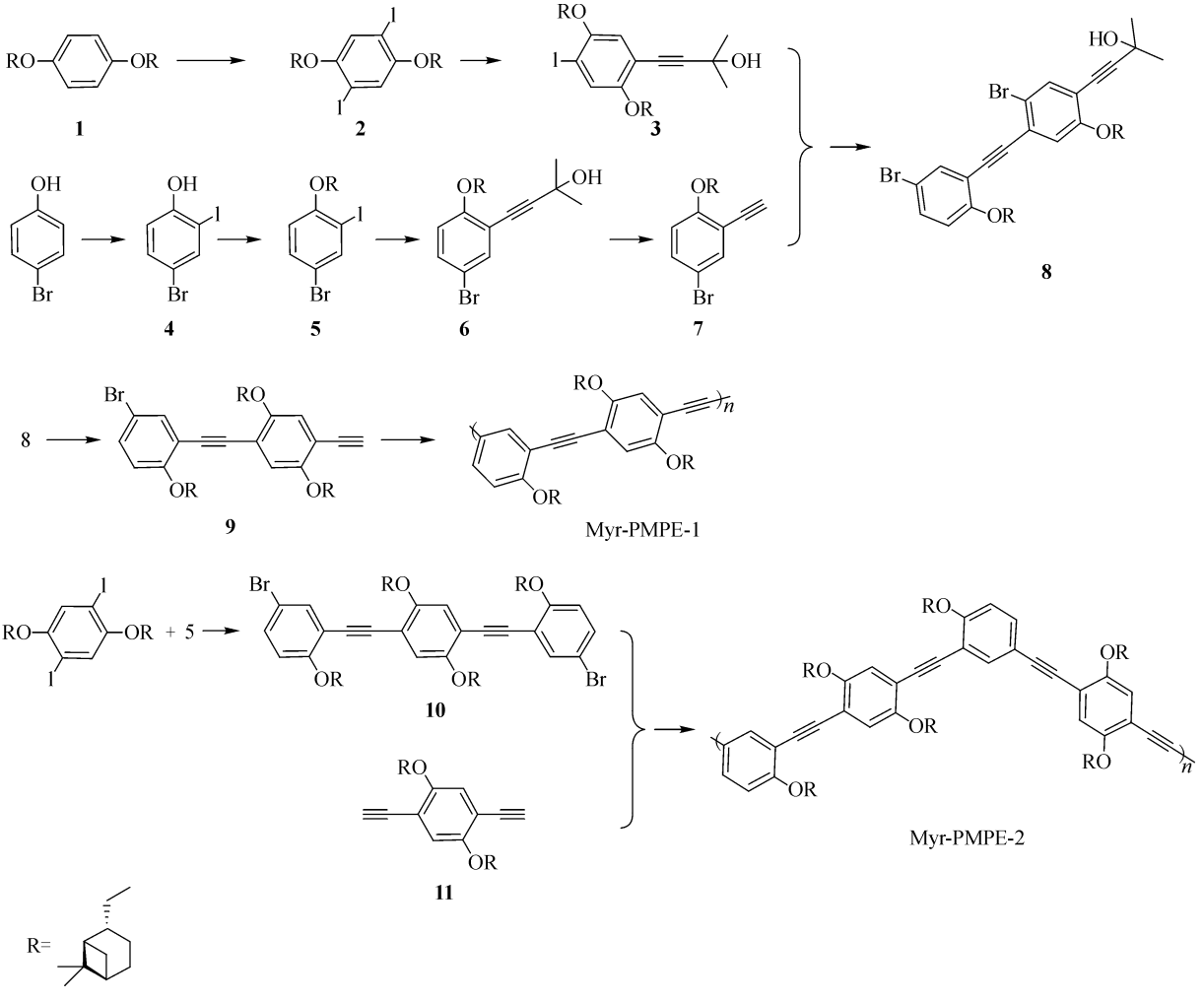

Scheme 1 Synthetic strategy of chiral regioregular poly(*p*-phenyleneethynylene-*alter*-*m*-phenyleneethynylene)

were carried out on a Netzsch DSC-204 differential scanning calorimeter (heating rate: 10 K/min; atmos.: N_2, 20.00 mL/min). Thermogravimetric analyses (TGA) were recorded on a Perkin-Elmer TGS-2 thermogravimeter (heating rate: 10 K/min; atmos.: N_2, 45.00 mL/min).

1.2 Pretreatments of materials and reagents

Dimethylsulfoxide (DMSO): dried overnight with anhydrous $MgSO_4$ and freshly distilled before use; Anhydrous tetrahydrofuran (THF) was freshly distilled from sodium and benzophenone before use. Triethylaimne (Et_3N): dried overnight with CaH_2 and freshly distilled before use. Other reagents were all reagent grade materials, purified by standard methods if needed.

1.3 General procedures of syntheses

(-)-*trans*-Myrtanyl tosylate [28], compound **4** [33] and compound **11** [28] were synthesized based on the references respectively.

1.3.1 Synthesis of compound **1**

Under the positive pressure of nitrogen, a solution of (-)-*trans*-myrtanyl tosylate (12.9 g, 42 mmol) in DMSO (25 mL) was added dropwise to a solution of hydroquinone (2.20 g, 20.0 mmol) and powdered KOH (3.36 g, 60 mmol) in DMSO (35 mL). The resulting mixture was stirred at room temperature overnight. Then, the contents were poured into water and extracted twice with ether. The combined extracts were washed with 10% NaOH solution, water and saturated NaCl solution successively, dried with anhydrous Na_2SO_4 and then filtered. The solvent was removed by rotary evaporation. The crude product was purified by recrystallization from $CHCl_3/CH_3OH$ (5.90 g, 77.1%). ^{1}H-NMR: δ 0.88(s, 6H), 1.23(s, 6H), 1.27–1.41(m, 4H), 1.66–2.11(m, 12H), 2.44(quint, J = 7.8 Hz, 2H), 3.67(d, J = 6.9 Hz, 4H), 6.78(s, 4H); Anal. Calcd: $C_{26}H_{38}O_2$, C 81.62, H 10.01, found C 81.62, H 9.79. EI MS m/z Calcd.: 382.29; found: 382.

1.3.2 Synthesis of compound **2**

A mixture of **1** (5.74 g, 15 mmol), I_2 (3.41 g, 13.5 mmol), HIO_3 (1.58 g, 9 mmol), 30% H_2SO_4 (4.5 mL) and CCl_4 (6 mL) in acetic acid (27 mL) was stirred under N_2 at 75°C for 6 h. Then, the mixture was poured into water and extracted twice with ether. The combined extracts were washed with 10% $Na_2S_2O_3$ solution, water and saturated NaCl solution successively, dried with anhydrous Na_2SO_4 and then filtered. The solvent was removed by rotary evaporation. The crude product was purified by recrystallization from $CHCl_3/CH_3OH$ after being chromatographed on silica gel with 5% ethyl acetate in petroleum ether (7.48 g, 78.5%): mp 109–110°C ^{1}H-NMR (300 MHz) :δ 0.89 (s, 6 H), 1.24 (s, 6 H), 1.35–1.50 (m, 4 H), 1.70–1.95 (m, 8 H), 1.96–2.16 (m, 4 H), 2.50 (quint, J = 7.5 Hz, 2 H), 3.65–3.74 (m, 4 H), 7.13 (s, 2 H). Anal. Calcd.: $C_{26}H_{36}I_2O_2$, C 49.23, H 5.72; found C 49.09, H 5.61. EI MS m/z Calcd.: 634.08; found: 634.

1.3.3 Synthesis of compound **3**

2.54 g of **2**, 28 mg of $Pd(PPh_3)_2Cl_2$ and 10 mg of triphenylphosphine were added to a two-necked flask. The flask was vacuumed and refilled with N_2. This process was repeated three times. 10 mL of THF was added, the mixture was stirred for 5 min. Then, 19 mg of CuI, 2.5 mL of Et_3N and 0.46 mL of 2-methylbut-3-yn-2-ol were added under N_2 successively. The resulting mixture was stirred at room temperature for 24 h. The reaction mixture was filtered through a short column of silica gel. The solvent in the filtrate was removed by rotary evaporation. The product was chromatographed on silica gel with 5% ethyl acetate in petroleum ether (1.15 g, 48.7%). ^{1}H-NMR (300 MHz) : δ 0.88 (s, 3H), 0.89(s, 3H), 1.23 (s, 3H), 1.24 (s, 3H), 1.30–1.50 (m, 4 H), 1.62 (s, 6H), 1.70–1.95 (m, 8 H), 1.96–2.10 (m, 4 H), 2.48 (quint, J = 7.2 Hz, 2 H), 3.65–3.74 (m, 4 H), 6.761 (s, 1H), 7.21 (s, 1H); Elem. Anal. Calcd.: $C_{31}H_{43}IO_3$, C 63.05, H 7.34, found C 63.34, H 7.406. FAB MS m/z calcd.: 590.23; found: 590.

1.3.4 Synthesis of compound **5**

A solution of (-)-*trans*-myrtyl tosylate (4.89 g, 12.8 mmol) in DMSO (15 mL) was added dropwise to a solution of **4** (3.00 g, 10.0 mmol) and powdered KOH (0.84 g, 15 mmol) in DMSO (15 mL) under N_2. The resulting mixture was stirred at room temperature overnight. Then, the contents were poured into water and extracted twice with ether. The combined extracts were washed with 10% NaOH solution, water and saturated NaCl solution successively, dried with anhydrous Na_2SO_4 and then filtered. The solvent was removed by rotary evaporation. The crude product was purified by chromatography on silica gel with petroleum ether to afford clear oil (2.59 g, 59.5%). ^{1}H-NMR: δ 0.89 (s, 3H), 1.24 (s, 3H), 1.35–1.50 (m, 2H), 1.65–2.15 (m, 6H), 7.51 (quint, J = 7.5 Hz, 1H), 3.65–3.85 (m, 2H), 6.61 (d, J = 8.7 Hz, 1H), 7.32 (dd, J_1 = 2.1 Hz, J_2 = 8.7 Hz, 1H), 7.82 (d, J = 2.1 Hz, 1H). Elem. Anal. Calcd.: $C_{16}H_{20}BrIO$, C 44.16, H 4.63; found C 44.39, H 4.732. FAB MS m/z calcd.: 433.97; found: 434.

1.3.5 Synthesis of compound **6**

4.35 g of **5**, 70 mg of $Pd(PPh_3)_2Cl_2$, and 26 mg of triphenylphosphine were added to a two-necked flask. The flask was vacuumed and then refilled with N_2. This process was repeated three times. Then, 47.5 mg of CuI, 15 mL of THF, 2 mL of Et_3N and 1.1 mL of 2-methylbut-3-

yn-2-ol were added under N_2 successively. The resulting mixture was stirred at room temperature for 5 h. The reaction mixture was filtered through a short column of silica gel. The solvent in the filtrate was removed by rotary evaporation. The crude product was purified by chromatography on silica gel with 5% ethyl acetate in petroleum ether to afford pale yellow crystals (3.52 g, 90.0%). ^{1}H-NMR (300 MHz): δ 0.88 (s, 3 H), 1.23 (s, 3 H), 1.30 –1.50 (m, 2 H), 1.61(s, 6 H), 1.65–1.95 (m, 4 H), 2.00–2.15 (m, embed a single, 2 H), 2.52 (quint, J = 7.50 Hz, 1 H), 3.65–3.80 (m, 2 H), 6.68 (d, J = 8.7 Hz, 1 H), 7.30 (dd, J_1 = 2.7 Hz, J_2 = 8.7 Hz, 1H), 7.44 (d, J = 2.4 Hz, 1 H). Elem. Anal. Calcd.: $C_{21}H_{27}BrO_2$, C, 64.45; H, 6.95; found C, 64.41; H, 6.893. FAB MS m/z calcd.: 390.12; found: 390.

1.3.6 Synthesis of compound **7**

1.96 g (5 mmol) of **6** was resolved in 10 mL of THF and 5 mL of methanol, the resulted solution was degassed by bubbling nitrogen for 30 min. Then, 5.6 g (100 mmol) of powdered KOH was added. The resulting solution was refluxed gently overnight. The reaction mixture was treated with saturated aq. NH_4Cl solution and then extracted with ethyl acetate twice. The combined extracts were washed with water and saturated NaCl solution successively, dried with anhydrous Na_2SO_4 and then filtered. The solvent was removed by rotary evaporation. The crude product was purified by chromatography on silica gel with petroleum ether. The product was crystallized overnight to afford white crystals (1.40 g, 84.0%). ^{1}H-NMR (300 MHz) : δ 0.87 (s, 3 H), 1.23 (s, 3 H), 1.30–1.50 (m, 2 H), 1.64–1.93 (m, 4 H), 1.94–2.14 (m, 2 H), 2.50 (quint, J = 7.50 Hz, 1 H), 3.26 (s, 1H), 3.70–3.85 (m, 2 H), 6.70 (d, J = 9 Hz, 1 H), 7.33 (dd, J_1 = 2.4 Hz, J_2 = 8.7 Hz, 1H), 7.50 (d, J = 2.4 Hz, 1H). Elem. Anal. Calcd.: $C_{18}H_{21}BrO$, C, 64.87; H, 6.35; found C, 64.95; H, 6.438. FAB MS m/z calcd.: 332.08; found: 332.

1.3.7 Synthesis of compound **8**

1.18 g of **3**, 0.80 g of **7**, 14 mg of $Pd(PPh_3)_2Cl_2$, 9.6 mg of CuI and 5.2 mg of triphenylphosphine were added to a two-necked flask. The flask was vacuumed and then refilled with N_2. This process was repeated three times. Then, 7.5 mL of THF and 2.5 mL of Et_3N were added. The resulting solution was stirred at room temperature for 24 h. The reaction mixture was filtered through a short column of silica gel. The filtrate was concentrated on the rotary evaporator, poured into methanol and then cooled to precipitate. After filtration, the obtained solids were chromatographed on silica gel with 5% ethyl acetate in petroleum ether to afford pale yellow crystals (1.16 g, 73.0%). ^{1}H-NMR: δ 0.88 (s, 3H), 0.89 (s, 3H), 0.91 (s, 3H), 1.21 (s, 3H), 1.23 (s, 3H), 1.24 (s, 3H), 1.30–1.55 (m, 6H), 1.63 (s, 6H), 1.65–1.95 (m, 12H), 2.00–2.15 (m, 6H), 2.45–2.60 (m, 3H), 3.65–3.85 (m, 6H), 6.72 (d, J = 9.0 Hz, 1H), 6.87 (s, 1H), 6.89 (s, 1H), 7.32 (dd, J_1 = 2.4 Hz, J_2 = 9.0 Hz, 1H), 7.52 (d, J = 2.4 Hz, 1H). Elem. Anal. Calcd.: $C_{49}H_{63}BrO_4$, C, 73.94; H, 7.98; found C, 73.88; H, 7.953. FAB MS m/z calcd.: 794.39; found: 795.

1.3.8 Synthesis of compound **9**

1.20 g (1.5 mmol) of **8** was dissolved in a mixture of 20 mL of THF and 5 mL of methanol. Then, 1.68 g (30 mmol) of powdered KOH was added. The resulting solution was refluxed gently overnight. The reaction mixture was treated with saturated aq. NH_4Cl solution and then extracted with ethyl acetate twice. The combined extracts were washed with water and saturated NaCl solution successively, dried with anhydrous Na_2SO_4 and then filtered. The solvent was removed by rotary evaporation. The crude product was purified by chromatography on silica gel with petroleum ether to afford pale yellow crystals (0.95 g, 85.8%). ^{1}H-NMR: δ 0.88 (s, 6H), 0.91 (s, 3H), 1.21 (s, 3H), 1.23 (s, 6H), 1.30–1.55 (m, 6H), 1.65–1.95 (m, 12H), 2.00–2.15 (m, 6H), 2.45–2.60 (m, 3H), 3.32 (s, 1H), 3.65–3.85 (m, 6H), 6.73 (d, J = 9.0 Hz, 1H), 6.91 (s, 1H), 6.94 (s, 1H), 7.32 (dd, J_1 = 2.4 Hz, J_2 = 9.0 Hz, 1H), 7.53 (d, J = 2.4 Hz, 1H). Elem. Anal. Calcd.: $C_{46}H_{57}BrO_3$, C, 74.88; H, 7.79; found C, 74.70; H, 7.822. FAB MS m/z calcd.: 736.35; found: 737.

1.3.9 Synthesis of Myr-PMPE-1

To a 25 mL two-necked flask, 0.74 g (1 mmol) of **9**, 0.0462 g (0.04 mmol) $Pd(PPh_3)_4$ and 0.0152 g (0.08 mmol) of CuI were added. The flask was vacuumed for 5 min and refilled with N_2. This process was repeated three times. A mixture of 25 mL of toluene and 10 mL of diisopropylamine, degassed by bubbling N_2 for 45 min, was added to the flask. The reaction mixture was stirred at 50°C for 48 h. Then, the reaction contents were poured into methanol. The products were collected by filtration and purified by being redissolved in THF and then precipitated in methanol (0.36 g, 55%). M_n = 2030, PDI = 1.13.

1.3.10 Synthesis of compound **10**

2.35 g of **2**, 2.45 g of **5**, 43.2 mg of $Pd(PPh_3)_2Cl_2$, 29.5 mg of CuI and 16.0 mg of triphenylphosphine were added to a two-necked flask. The flask was vacuumed and then refilled with N_2. This process was repeated three times. Then, 25 mL of THF and 10 mL of Et_3N were added. The resulting solution was stirred at room temperature for 24 h. The reaction mixture was filtered through a short column of silica gel. The filtrate was concentrated on a rotary evaporator, poured into methanol and then cooled to precipitate. After filtration, the obtained solids were chromatographed on silica gel with 5% ethyl acetate in

petroleum ether to afford pale yellow crystals (0.97 g, 40%). ^{1}H-NMR: δ 0.91 (s, 6H), 0.94 (s, 6H), 1.24 (s, 6H), 1.26 (s, 6H), 1.58–1.37 (m, 8H), 1.98–1.67 (m, 16H), 2.17–2.02 (m, 8H), 2.64–2.46 (m, 4H), 3.90–3.70 (m, 8H), 6.75 (d, J = 9.0 Hz, 2H), 6.95 (s, 2H), 7.34 (dd, J_1 = 2.4 Hz, J_2 = 8.7 Hz, 2H), 7.53 (d, J = 2.4 Hz, 2H). Elem. Anal. Calcd.: $C_{62}H_{76}Br_2O_4$, C, 71.25; H, 7.33; found C, 73.13; H, 7.529. FAB MS m/z calcd.: 1042.41; found: 1043.

1.3.11 Synthesis of Myr-PMPE-2

To a 25 mL two-necked flask, 0.72 g(0.69 mmol) of **10**, 0.315 g (0.69 mmol) of **11**, 0.022 g (0.028 mmol) $Pd(PPh_3)_4$ and 10.5 mg (0.056 mmol) of CuI were added. The flask was vacuumed for 5 min and refilled with N_2. This process was repeated three times. A mixture of 25 mL of toluene and 10 mL of diisopropylamine, degassed by bubbling N_2 for 45 min, was added to the flask. The reaction mixture was stirred at 75°C for 96 h. Then the reaction contents were poured into methanol. The products were collected by filtration and purified by being redissolved in THF and then precipitated in methanol (0.74 g, 80.4%). M_n = 7030, PDI = 2.65.

1.4 Preparation and annealing of the polymer films

The polymer films were obtained by spin-coating on glass substrates from a 10 mg/mL solution in toluene. The obtained films were annealed under N_2 for a desired time at designed temperature and slowly cooled to room temperature.

2 Results and discussion

2.1 Design and synthesis of the polymers

Based on the references, the design of the polymers was focused on the following points. (1) Synthesis of polymers with highly regular molecular structure. We have reported that it is hard to obtain highly regular polymers with Wittig reaction or Heck reaction [34,35], because both of them occur along with isomerization reactions and hence induce isomer structures in the polymer. In this paper, a Sonogashira reaction was selected to synthesize chiral polyphenyleneethynylene. (2) We have found that the introduction of an intrinsically helical structure by *m*-phenylne linkages can obviously enhance the optical activity compared to the polymer which adopts linear rod-like conformation [34]. In this paper, *m*-phenylene linkages were also introduced to synthesize poly(*p*-phenyleneethynylene-*alter*-*m*-phenyleneethynylene) which adopts intrinsically helical conformation. (3) Chiral side groups were introduced both in the *p*-phenylene ring and *m*-phenylene ring to increase the average number of chiral groups per monomeric unit. (4) Regioregular linking pattern between *p*-phenyleneethynylene monomeric unit and *m*-phenyleneethynylene monomeric unit. Since it is difficult to obtain symmetric chiral *m*-phenyleneethynylene monomer, and there will be two different linking patterns, e.g. head to head and head to tail, irregularly distributed in the polymer obtained by the polymerization of *p*-dihalobenzene and *m*-diethynylbenzene (Scheme 2).

It has been reported that such irregular polymer did not show optical activity [4, 30]. So, it is necessary to design monomer structure to ensure regularly linking between monomeric units.

Thus, based on the obviously different activity between bromo- and iodo-benzene in Sonogashira reaction, we designed and synthesized an AB-type monomer (compound **9** in Scheme 1) containing ethynyl group in one end and bromo-group in another end by stoichiometric control. ^{1}H-NMR spectrum of the monomer (compound **9**) and its peak assignments are shown in Fig. 1(a).

Obviously, the linking pattern of monomeric unit is unique in the polymer obtained by the AB-type monomer, so the structure of the polymer is regular. ^{1}H-NMR spectrum of the obtained polymer (Myr-PMPE-1) and its peak assignments are shown in Fig. 1(b).

By the same strategy, we designed and synthesized a symmetric AA-type dibromo- monomer (compound **10**).

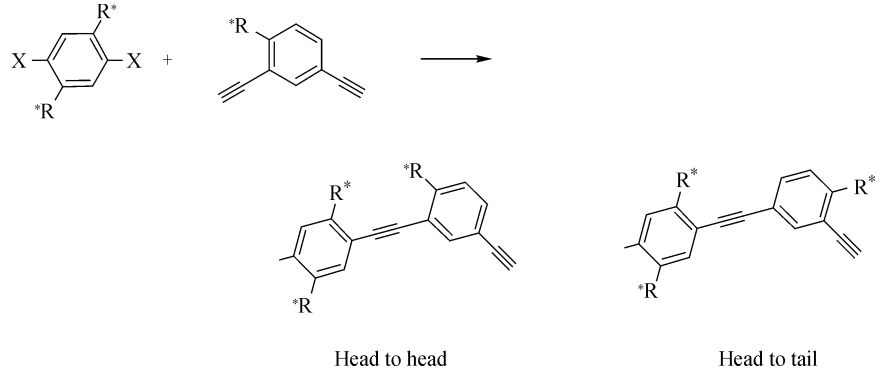

Scheme 2 Different linking patterns of monomer units in irregular polymer

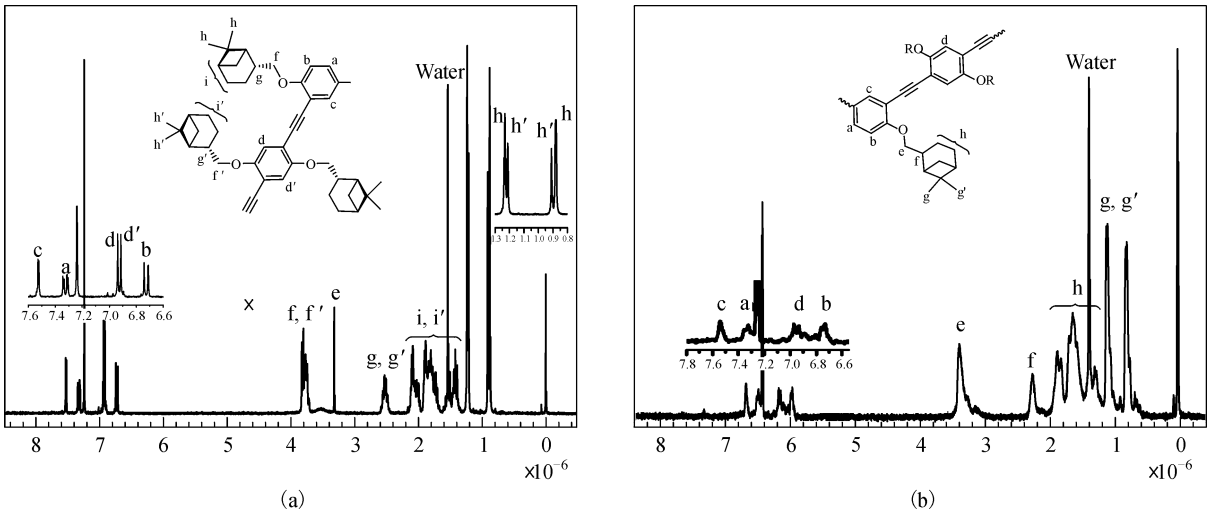

Fig. 1 [1]H-NMR spectra of compound 9 (**a**) and Myr-PMPE-1 (**b**)

The AA + BB polymerization of compound **10** with another symmetric diethynyl- monomer (compound **11**) will also give regioregular polymer. [1]H-NMR spectra of compound **10** and the corresponding polymer (Myr-PMPE-2) are shown in Fig. 2(a) and (b).

Both of Myr-PMPE-1 and Myr-PMPE-2 are oligomers with relatively low molecular weight (Myr-PMPE-1: M_n = 2030, PDI = 1.13; Myr-PMPE-2: M_n = 7030, PDI = 2.65). These two polymers have the same chemical component and main chain structure, but the substitution pattern of the chiral groups is different from each other. In Myr-PMPE-1, the side chiral groups are distributed uniformly along the backbone. As shown in Scheme 3, the chiral group on *m*-phenylene is always regularly located at the *p*- or *m*-position to the *p*-phenylene. The molecular structure is highly symmetric. But in Myr-PMPE-2, the distribution of the side chiral groups is alternatively crowded and loose. For the *p*-phenylene in the dashed circle, the chiral groups on the neighbor *m*-phenylenes are both located on the *m*-position, so, in this locale, the distribution of chiral groups are relatively "crowded". For the other *p*-phenylene, the chiral groups on the neighbor *m*-phenylenes are both located on the *p*-position. Thus, the distribution of chiral groups are relatively "loose" in this locale. The symmetry of its molecular structure is lower than that of Myr-PMPE-1.

2.2 Properties of the polymers

Both Myr-PMEP-1 and Myr-PMPE-2 have good solubility in common organic solvents, and show no optical activity in a good solution. But due to their good solubility, it is easy to obtain fine film by spin-coating. Therefore, the investigations of chiroptical properties of the polymers were carried out on solid films.

It is well known that polymer chains can reorganize by segmental motion under annealing over the glass tempera-

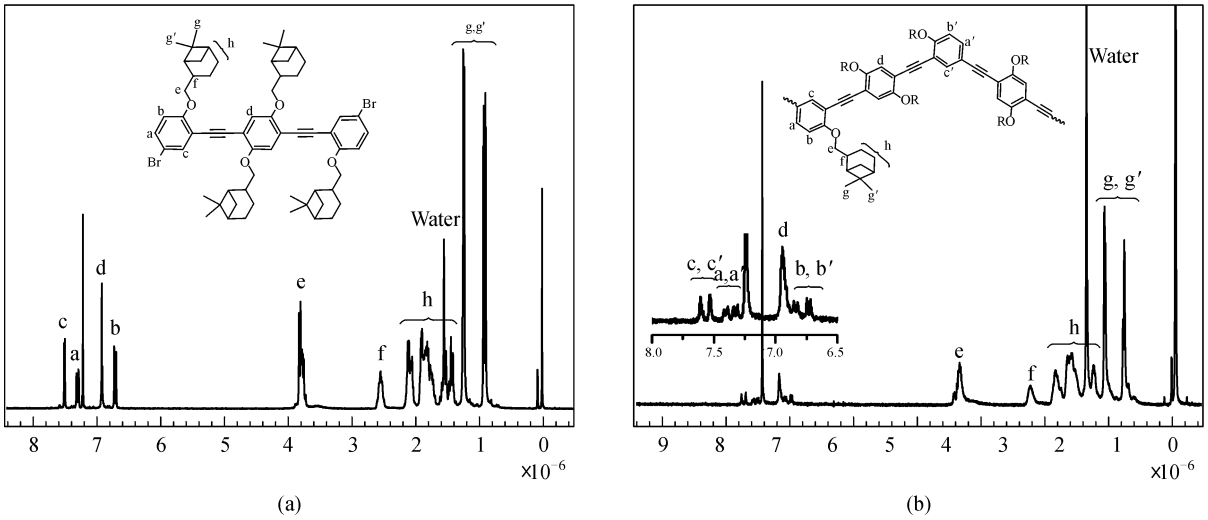

Fig. 2 [1]H-NMR spectra of compound 10 (**a**) and Myr-PMPE-2 (**b**)

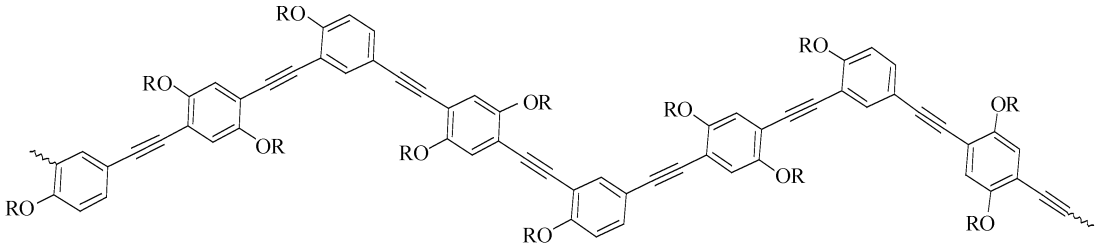

Myr-PMPE-1

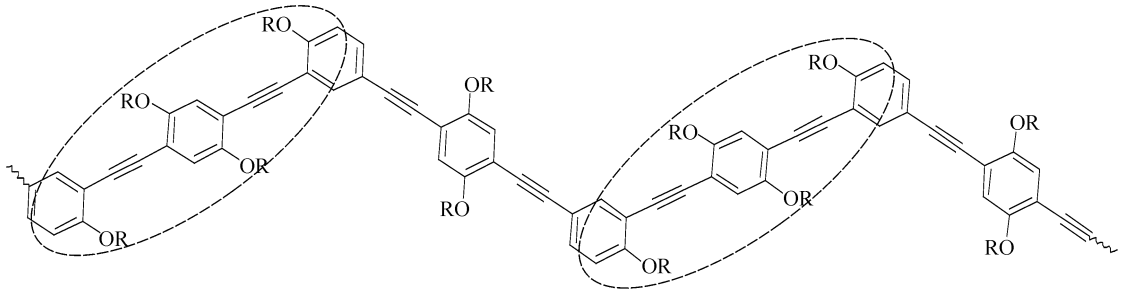

Myr-PMPE-2

Scheme 3 Comparison of the molecular structures of Myr-PMPE-1 and Myr-PMPE-2

ture (T_g) of the polymer. By annealing over T_g, conjugated polymers bearing flexible side groups can change the disordered phase, which resulted from spin-coating, into ordered phase by reorganization [36]. In order to investigate the effect of annealing treatment on the optical activity of the obtained polymers, the thermal properties of the polymers were first investigated.

2.2.1 Thermal properties of Myr-PMPE-1 and Myr-PMPE-2

TGA and DSC measurements were carried out to investigate the thermal properties of Myr-PMPE-1 and Myr-PMPE-2. The TGA curves and DSC curves are shown in Figs. 3 and 4, respectively. For Myr-PMPE-1, the onset of weight loss is at 272°C, and the weight loss of 5% occurs at 320°C. For Myr-PMPE-2, the onset of weight loss is at 340°C, and the weight loss of 5% occurs at 360°C. Therefore, both of them have relatively good thermal stability. The glass temperatures (T_g) are 85°C and 89°C for Myr-PMPE-1 and Myr-PMPE-2, respectively. So, the annealing temperature was selected to range between 80–140°C.

2.2.2 Chiroptical properties of the polymer films

The original and normalized UV-Vis absorption spectra of Myr-PMPE-1 film annealed under different temperatures are shown in Fig. 5.

The original spectra show that the absorption intensities decrease with increasing annealing temperature, and as

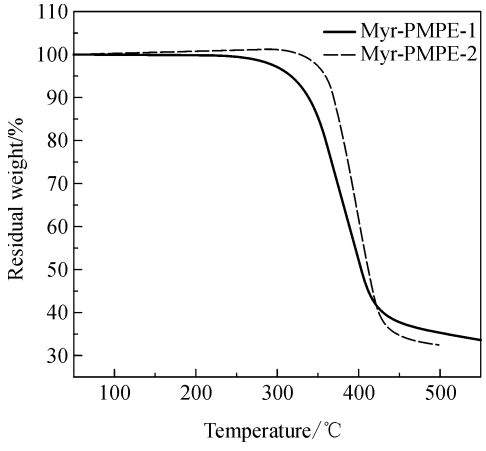

Fig. 3 TGA curves of Myr-PMPE-1 and Myr-PMPE-2

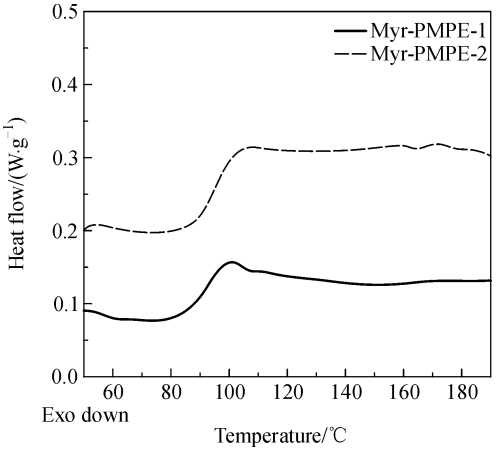

Fig. 4 DSC curves of Myr-PMPE-1 and Myr-PMPE-2

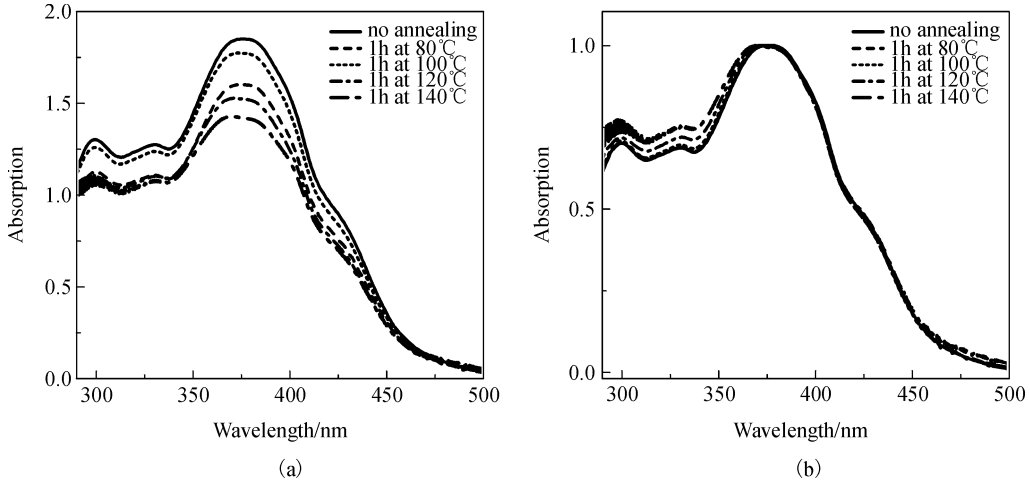

Fig. 5 Effect of annealing on the UV-Vis spectra of Myr-PMPE-1 film (**a**) Original; (**b**) Normalized

shown in the normalized spectra (Fig. 5(b)), the spectra are almost identical in the range at longer wavelength (>375 nm), but the relative intensities of the bands in the range at shorter wavelength (<375 nm) slightly increase with increasing annealing temperature, and similar to the chiral polythiophylenevinylene (BMB-PTV) reported by Cronelissen *et al.* [18], the maximum absorptions are slightly blue-shifted. The normalized emission spectra of Myr-PMPE-1 film before and after annealing are shown in Fig. 6. The emission spectrum shows no significant change before and after annealing, except that the relative intensity of the shoulder peak at around 530 nm slightly increases. These results indicate that annealing treatment did not significantly affect the aggregation structure of Myr-PMPE-1 films.

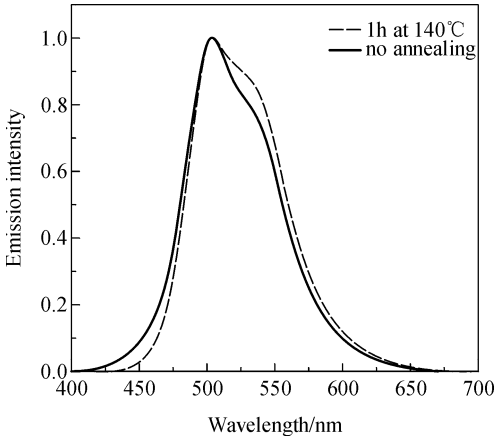

Fig. 6 Normalized emission spectra of a Myr-PMPE-1 spin-coated films before and after annealing, excited at 383 nm

The effects of annealing on the CD spectra and maximum g value (g_{max}) of the Myr-PMPE-1 film are shown in Fig. 7 and Table 1, respectively. Figure 7 shows that the intensities of CD signals decrease with increasing annealing temperature, similar to the change of UV-Vis spectra, and the $|g_{max}|$ value shows no significant change.

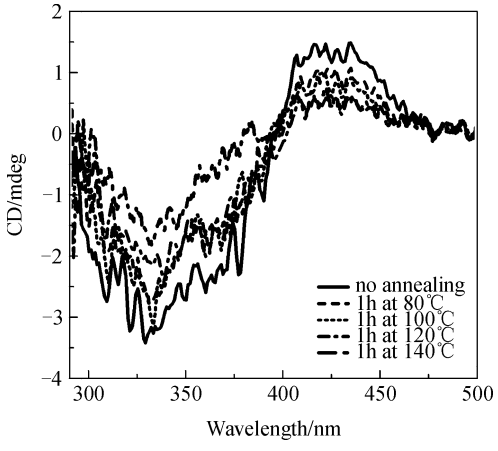

Fig. 7 CD spectra of Myr-PMPE-1 spin-coated films annealed at different temperatures

The original and normalized UV-Vis absorption spectra of Myr-PMPE-2 films annealed under different temperatures are shown in Fig. 8. Similar to the spectra of Myr-PMPE-1, the absorption intensities decrease with increasing annealing temperature. As shown in the normalized spectra (Fig. 8(b)), the relative intensities of the bands in the range at shorter wavelength (<375 nm) slightly increase with increasing annealing temperature, and the max keeps unchanged. However, the intensity of the shoulder peak at around 425 nm increases obviously, and consequently, the λ_{max} at the range of longer wavelength shows a slight red-shift. The normalized emission spectra of Myr-PMPE-2 films before and after annealing are shown in Fig. 9. The max of the emission band shows an obvious red-shift from 514 nm to 534 nm. Based on the analysis of UV-Vis absorption and emission spectra, it can

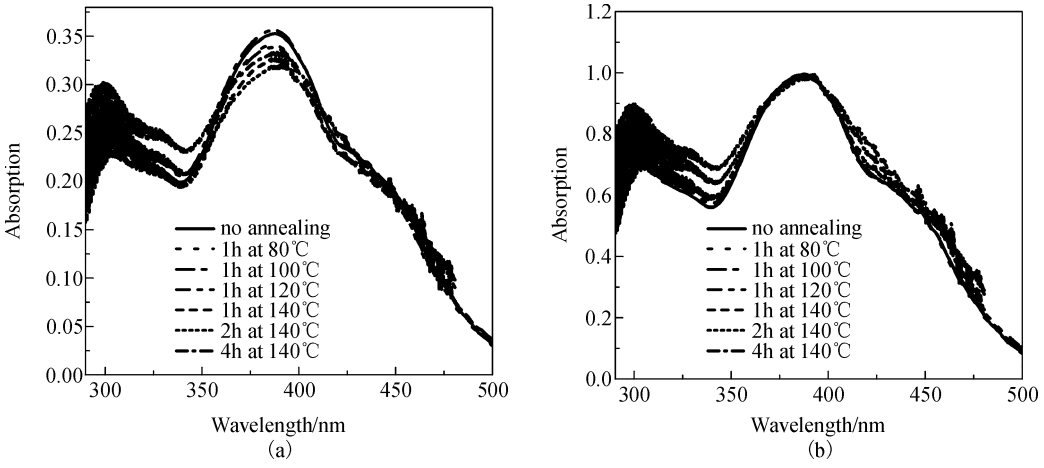

Fig. 8 Effect of annealing on the UV-Vis spectra of Myr-PMPE-2 films

be concluded that the aggregation structure of Myr-PMPE-2 film has been changed markedly after annealing. Under annealing temperature, the polymer chains can reorganize into an ordered structure and aggregate tightly. This can lead to an enhancement of the interchain interaction and make the energy bands of conjugation segments widen to decrease the band gaps [37,38]. Therefore, the UV-Vis absorption and emission spectra are red-shifted. Similar changes can also be observed in the CD spectra.

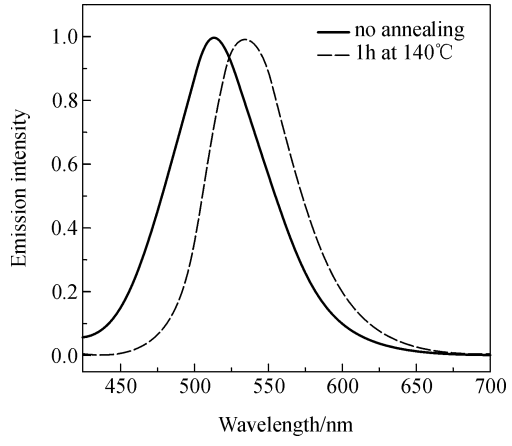

Fig. 9 Normalized emission spectra of Myr-PMPE-2 spin-coated films before 4 and after annealing, excited at 398 nm

The effects of annealing on the CD spectra and gmax value of Myr-PMPE-2 film are shown in Fig. 10 and Table 1, respectively. Different to Myr-PMPE-1 film, Myr-PMPE-2 film shows none or very weak signals in the CD spectra without annealing or annealing at lower temperature (⩽120°C). But the intensity of the CD signal markedly increases under annealing at 140°C. The intensity of the maximum CD signal increases from 8.36 $\times$ 10^{-4} mdeg under 120°C to 3.82 mdeg under 140°C, enhanced almost 4 orders of magnitude and continuously increases with increasing annealing time. The g_{max} value of Myr-PMPE-2 film before annealing is close to 0, but increases to 3 $\times$ 10^{-3} after annealing at 140°C for 4 h. More importantly, after annealing, the g_{max} value of Myr-PMPE-2 film is about one order of magnitude higher than that of Myr-PMPE-1.

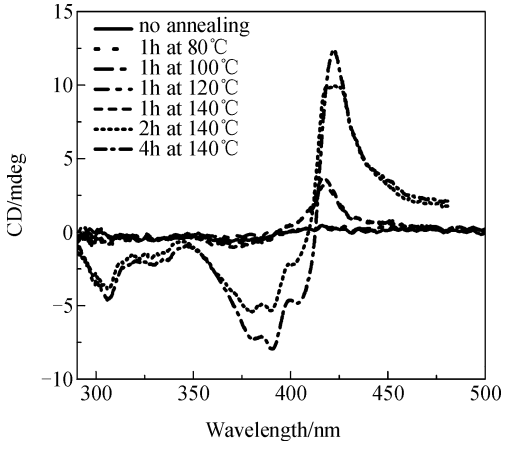

Fig. 10 CD spectra of a Myr-PMPE-2 spin-coated film on glass after annealing

Table 1 Effect of annealing on the g_{max} of Myr-PMPE-1 and Myr-PMPE-2

Annealing temperature	g_{max} in absorption/10^{-4}		
	Myr-PMPE-1	Myr-PMPE-2	
No annealing	−1.62	–	–
80°C	−1.52	–	–
100°C	−1.53	–	–
120°C	−1.18	8.36 (418 nm)	−1.15 (375 nm)
1 h at 140°C	−1.01	9.60 (418 nm)	−1.76 (373 nm)
2 h at 140°C		24.9 (423 nm)	−9.81 (390 nm)
4 h at 140°C		30.7 (421 nm)	−14.1 (390 nm)

The above results show that not only annealing treatment, but also the substitution pattern of the chiral side groups, has significant effects on the chiroptical properties of chirally substituted conjugated polymers. For Myr-PMPE-1, the polymer chains are easier to organize into ordered structures than Myr-PMPE-2 because of its higher molecular symmetry and shorter molecular chain. When spin-coated, Myr-PMPE-1 molecules can organize to a relatively high ordered aggregation state by the evaporation of solvents and the obtained film shows a certain extent of optical activity. Annealing treatment has no significant effect on the order of aggregation structure, and hence, has no obvious effect on its optical activity. For Myr-PMPE-2, due to its lower molecular symmetry and longer polymer chain, the segmental motion is more difficult than that of Myr-PMPE-1 and the polymer chains are fixed without enough time to relax during the spin-coating process. There are many conformational defects in the polymer chains, so the aggregation structure of Myr-PMPE-2 film is low ordered. As a result, the optical activity of the spin-coated film of Myr-PMPE-2 is very low. Under annealing above glass temperature, the polymer chains can relax to reduce the conformational defects and reorganize into ordered aggregation structure by segmental motion and the order of aggregation increases with increasing annealing temperature and time. Consequently, the optical activity of Myr-PMPE-2 films increases markedly. Because Myr-PMPE-1 and Myr-PMPE-2 have the same chemical components and main chain structure, the higher optical activity of annealed Myr-PMPE-2 films can be attributed to the different substitution pattern of the chiral groups. The results show that the substitution pattern of Myr-PMPE-2 is more favored to obtain high optical activity. The local "crowded" structure of chiral substituent in Myr-PMPE-2 makes the polymer chain easier to coil into helical conformation. This is similar to the chiral poly(*p*-phenylene-alter-2,5-furan) reported by Dubus *et al.* [39], which is more easily forms helical conformations when the chiral substituents are located in a crowded substitution pattern, and it has been reported that the formation of helical conformation can obviously increase the optical activity [31,34].

3 Conclusion

Two regioregular poly(*p*-phenyleneethynylene-*alter*-*m*-phenyleneethynylene)s bearing (-)-*trans*-myrtanoxyl side groups with different substitution patterns were designed and synthesized. In Myr-PMPE-1, the side chiral groups were distributed uniformly along the backbone. While in Myr-PMPE-2, the distribution of the side chiral groups was alternatively crowded and loose. The effects of annealing temperature and time on the properties of the films were investigated by UV-Vis absorption, fluorescence and circular dichroism spectra. The results show that annealing treatment had no significant effect on the properties of Myr-PMPE-1. On the other hand, annealing treatment significantly affected the properties of Myr-PMPE-2. When annealed above 120°C, the absorption and emission of Myr-PMPE-2 film red shifted slightly with increasing annealing temperature and annealing time, and the optical activity increased obviously. After annealing at 140°C for 4 h, $|g_{max}|$of the Myr-PMPE-2 film was up to 3.07×10^{-3}, about one order of magnitude higher than that of the Myr-PMPE-1 film. These observations indicate that the substitution pattern of the chiral side groups has significant effect on the chiroptical properties of chirally substituted conjugated polymers. The obtained results can contribute to the design of chiral conjugated polymers with high optical activity.

Acknowledgements Project 50103013 supported by the National Natural Science Foundation of China and Team Project 039184 supported by the Natural Science Foundation of Guangdong Province, China.

References

1. Gao H L, Knobler C M, Kaner R B. A chiral recognition polymer based on polyaniline. Synth Met, 1999, 101: 44–47
2. Shinohara K, Aoki T, Kaneko T, Oikawa E. Syntheses and enantioselective recognition of chiral poly(phenyleneethynylene)s bearing bulky optically active- menthyl groups. Polymer, 2001, 42: 351–355
3. Moutet J C, Saintaman E, Tranvan F, Angibeaud P, Utille J P. Poly (glucose- pyrrole) modified electrodes: A novel chiral electrode for enantioselective recognition. Adv Mater, 1992, 4: 511–513
4. Bross P A, Schoberl U, Daub J. Carbohydrate-modified conducting polymers synthesis and electrochemistry of sugar-linked azulenes polyazulenes. Adv Mater, 1991, 3: 198–200
5. Koeckelberghs G, Sioncke S, Verbiest T, Persoons A, Samyn C. Synthesis and properties of chiral helical chromophore functionalized polybinaphthalenes for second-order nonlinear optical applications. Polymer, 2003, 44: 3785–3794
6. Bouman M M, Meijer E W. Stereomutation in optically active regioregular polythiophenes. Adv Mater, 1995, 7: 385–387
7. Peeters E, Christiaans M P T, Jassen R A J, Schoo H F M, Dekkers H P J M, Meijer E W. Circularly polarized electroluminescence from a polymer light- emitting diode. J Am Chem Soc, 1997, 119: 9909–9910
8. Yan J G, Liang H, Lu J. Studies on the circularly polarized luminescent polymers. Polym Bull, 2002, 4: 26–31 (in Chinese)
9. Pu L. The study of chiral conjugated polymers. Acta Polym, 1997, 48: 116–141
10. Ma L, Hu Q S, Vitharanak D, Wu C, Kwan C M.S, Pu L. A new class of chiral conjugated polymers with a propeller-like structure. Macomolecules, 1997, 30: 204–218
11. Cheng H, Pu L. Synthesis of chiral conjugated propeller-like polymers using optically active 1,1'-binaphthyl-2,2'-diamine derivatives. Macromol Chem Phys, 1999, 200: 1274–1283

12. Liu T J, Zhang K S, Chen Y J, Wang D, Li C J. Chiral conjugated oligomer based on 1,1'-binol with 3,3'-acetylene acetylene spacer. Chinese J Polym Sci, 2001, 19: 521–526
13. Cheng Y X, Chen L W, Zou X W, Song J F. Synthesis of chiral conjugated polybinaphthyls by sonogashira reaction. Chinese J Polym Sci, 2006, 24: 273–279
14. Cheng Y X, Chen L W, Liu T D. Synthesis of polybinaphthyl incorporating chiral (R)-1,1'-bi-2,2'-naphthol entities wiyh *p*-divinylbenzene by Pd-catalyzed heck reaction. Chinese J Polym Sci, 2004, 22: 327–331
15. Langeveld-Voss M W, Janssen R A J, Christiaans M P T, Meskers S C J, Dekkers H P J M, Meijer E W. Circular dichroism and circular polarization of photoluminescence of highly ordered poly{3,4-di[(S)-2-methylbutoxy]thiophene}. J Am Chem Soc, 1996, 118: 4908–4909
16. Andreani F, Angiolini L, Caretta D, Salatelli E. Synthesis and polymerization of 3,3"-di[(S)-(+)-2-methylbutyl]-2,2':5',2"-terthiophene: a new monomer precursor to chiral regioregular poly (thiophene). J Mater Chem, 1999, 8: 1109–1111
17. Meskers S S J, Langeveld-Voss B M W, Janssen R A J. Circular polarization of the fluorescence from films of poly(*p*-phenylene vinylene) and polythiophene with chiral side chains. Adv Mater, 2000, 12: 589–594
18. Cornelissen J J L M, Peeters E, Janssen R A J, Meijer E W. Chiroptical properties of a chiral-substituted poly(thienylenevinylene). Acta Polym, 1998, 49: 471–476
19. Peeters E, Delmotte A, Janssen R A J, Meijer E W. Chiroptical properties of poly{2, 5-bis[(S)-2-methylbutoxy]-1, 4-phenylene vinylene}. Adv Mater, 1997, 9: 493–496
20. Peeters E, Janssen R A J, Meijer E W. Effect of intrachain order on the chiroptical properties of chiral poly(*p*-phenylene vinylenes). Synth Met, 1999, 102: 1105–1106
21. Oda M, Nothofer H G, Lieser G, Scherf U, Meskers S C J, Neher D. Circularly polarized electroluminescence from liquid-crystalline chiral polyfluorenes. Adv Mater, 2000, 12: 362–365
22. Oda M, Meskers S C J, Nothofer H G, Scherf U, Neher D. Chiroptical properties of chiral-substituted polyfluorenes. Synth Met, 2000, 111–112: 575–577
23. Oda M, Nothofer H G, Scherf U, Sunjic V, Richter D, Regenstein W, Neher D. Chiroptical properties of chiral substituted polyfluorenes. Macromolecules, 2002, 35: 6792–6798
24. Lai L M, Lam J W Y, Tang B Z. Synthesis and chiroptical properties of L-valine-containing poly(phenylacetylene)s with (a)chiral pendant terminal groups. J Polym Sci Part A: Polym Chem, 2006, 44: 2117–2129
25. Lai L M, Lam J W Y, Tang B Z. Facile synthesis and high optical activity of poly(1-pentyne)s carrying amino-acid pendant groups. J Polym Sci Part A: Polym Chem, 2006, 44: 6190–6201
26. Toyoda S, Fujiki M. Experimental evidence for helical conformation of poly(methylphenylsilylene) in solution. Chem Lett, 1999, 28: 699–700
27. Koe J R, Fujiki M, Motonaga M, Nakashima H. Cooperative helical order in optically active poly(diarylsilylenes). Macromolecules, 2001, 34: 1082–1089
28. Cheng Y J, Liang H, Luh T Y. Chiral silylene-spaced divinylarene copolymers. Macromolecules, 2003, 36: 5912–5914
29. Zhang Z B, Motonaga M, Fujiki M, McKenna C E. The first optically active polycarbazoles. Macromolecules, 2003, 36: 6956–6958
30. Bouman M M, Havinga E E, Jassen R A J, Meijer E W. Chiroptical properties of regioregular chiral polythiophenes. Mol Cryst Liq Cryst, 1994, 256: 439–448
31. Langeveld-Voss B M W, Beljonne D, Shuai Z, Janssen R A J, Meskers S C J, Meijer E W, Brédas J-L. Investigation of exciton coupling in oligothiophenes by circular dichroism spectroscopy. Adv Mater, 1998, 10: 1343–1348
32. Curran S A, Ajayan P M, Blau W J, Carroll D L, Coleman J N, Dalton A B, Davey A P, Drury A, McCarthy B, Maier S, Strevens A. A composite from poly(*m*-phenylenevinylene-co-2,5-dioctoxy-*p*-phenylenevinylene) and carbon nanotubes: A novel material for molecular optoelectronics. Adv Mater, 1998, 10: 1091–1093
33. Cowart M, Faghih R, Curtis M P, Gfesser G A, Bennani Y L, Black L A, Pan L, Marsh K C, Sullivan J P, Esbenshade T A, Fox G B, Hancock A A. 4-(2-[2-(2(R)-Methylpyrrolidin-1-yl)ethyl] benzofuran-5-yl)benzonitrile and related 2-aminoethylbenzofuran H3 receptor antagonists potently enhance cognition and attention. J Med Chem, 2005, 48: 38–55
34. Li X, Li C, Yan J, Lu J, Liang H. Synthesis and chiroptical properties of poly (*p*-phenylenevinylene-*alter*-*m*-phenylenevinylene) bearing (-)-*trans*-myrtanoxyl groups on the *p*-phenylene rings. J Polym Sci Part A: Polym Chem, 2008, 46: 3336–3343
35. Yan J, Lu J, Liang H. Synthesis and properties of poly(*m*-phenylenevinylene). Acta Polym Sin, 2004, 3: 434–438 (in Chinese)
36. Asada K, Kobayashi T, Naito H. Temperature dependence of photoluminescence in polyfluorene thin films—Huang–Rhys factors of as-coated, annealed and crystallized thin films. Thin Solid Films, 2006, 499: 192–195
37. Kong F, Zhang S Y, Yang C Z, Yuan R K. Interchain excited states in annealed poly[2-methoxy-5-(2'-ethyl-hexyloxy)-*p*-phenylene vinylene] films. Mater Lett, 2006, 60: 3887–3890
38. Tretiak S, Saxena A, Martin R L, Bishop A R. Interchain electronic excitations in poly(phenylenevinylene) (PPV) aggregates. J Phys Chem B, 2000, 104: 7029–7034
39. Dubus S, Marceau V, Leclerc M. Helical conjugated polymers by design. Macromolecules, 2002, 35: 9296–9299